 ©2004 Uspekhi Fizicheskikh Nauk, Russian Academy of Sciences

CONFERENCES AND SYMPOSIA

PACS number: 01.10.Fv

Physical Sciences Division session at the General meeting of the Russian Academy of Sciences (17 May 2004)

On 17 May 2004, a general meeting of the Russian Academy of Sciences Physics Sciences Division was held in the conference room of the Lebedev Physics Institute. The fifth item on the agenda was a session on ''The Physics of Nanostructures and Nanotechnologies''. The following talks were given:

1. **Alferov Zh I** (Ioffe Physico-Technical Institute, St. Petersburg) ''Nanostructures: physics, technology, and applications in electronics'';
2. **Timofeev V B** (Institute of Solid State Physics, Chernogolovka) ''Electron correlation phenomena in semiconductor low-dimension structures and nanostructures'';
3. **Gaponov S V** (Institute of Physics of Microstructures, N Novgorod) ''Nanolithography and advances in technology'';
4. **Koval'chuk M V** (Shubnikov Institute of Crystallography) ''Bioorganic materials, structures, and diagnostics''.

A short version of talk No. 2 is available below.

PACS numbers: **71.35.–y**, **71.36.+c**, **73.43.–f**, **73.63.–b**
DOI: 10.1070/PU2004v047n10ABEH001929

Electron correlation phenomena in semiconductor low-dimension structures and nanostructures

V B Timofeev

1. Introduction

The most remarkable electronic phenomena in low-dimension semiconductor systems are those related to electron correlations. In such systems, spatial constraints (or quantum confinements) force particles closer together, increasing the effects of the exchange and correlation interactions. When a strongly interacting system is dimensionally reduced, fundamentally new gauge fields arise (the Chern–Simons gauge field, for example). Electron correlations underlie new phenomena and give rise to unexpected and sometimes exotic electron phases in low-dimension semiconductor systems. For systems with one-dimensional quantum confinement, examples are: a two-dimensional (2D) electron gas in a strong transverse magnetic field; spatially separated, 2D electron–electron and electron–hole layers; neutral and charged exciton complexes in quantum wells; and 2D exciton polaritons in microcavities. In systems with two-dimensional quantum confinement, a new quantum object, a Luttinger liquid, arises; a one-particle exciton in a quantum wire is a close analog of a diamagnetic exciton in an extremely strong magnetic field. In the case of three-dimensional quantum confinement, there arise artificially prepared atomic and molecular objects that have become widely known as quantum dots. Quantum dots can also form more complex molecular systems. It is these objects with which the latest breakthrough laser technologies are associated and which offer high hopes for practical applications in electronics and informatics and in the new and developing field of spintronics.

This fast growing area is one where fundamental scientific discoveries are strongly interwoven with technological advances. On the other hand, it is fundamental scientific discoveries that stimulated the practical implementation of fundamentally new ideas and provided a strong basis for true technology breakthroughs (examples, among many others, are selective (modulated) and delta doping techniques for heterostructures, and self-organized quantum dot growth at heteroboundaries). It is fair to say that major nanotechnology achievements are thoroughly imbued with ideas that came from basic research. The integration of and interplay between fundamental scientific and technological developments is and in the near future will be the determining factor in solid state electronics and informatics. The examples that argue in favor of this statement are many, and one of them, related to two-dimensional electrons, we will take some time to discuss here. The discovery, in the last quarter of the twentieth century, of new fundamental phenomena in the system of strongly interacting two-dimensional electrons became possible because of the impressive and continuous improvements the related low-dimensional semiconductor objects have obtained in terms of quality and structural perfection. Figure 1 gives an idea of the series of phenomena that have been successively discovered as the mobility and mean free path of two-dimensional electrons has increased (by more than three orders of magnitude!) in these systems. The electron mobility record for GaAs heterostructures is currently 3×10^7 cm^2 (V C)$^{-1}$, with mean free paths reaching 100 μm. The phenomena indicated at the upper right of the figure are those associated with composite fermions — a new class of quasiparticles that was discovered in structures with high electron mobility and is discussed immediately below.

2. Composite fermions

There are various ways to explain the concept of composite fermions pioneered by J K Jain [1]. Viewed phenomenologically, however, all of them ultimately reduce to a system of strongly interacting electrons in a sufficiently strong transverse magnetic field B transformed into a system of weakly

Uspekhi Fizicheskikh Nauk **174** (10) 1109 – 1117 (2004)
Translated by E G Strel'chenko; edited by A M Semikhatov

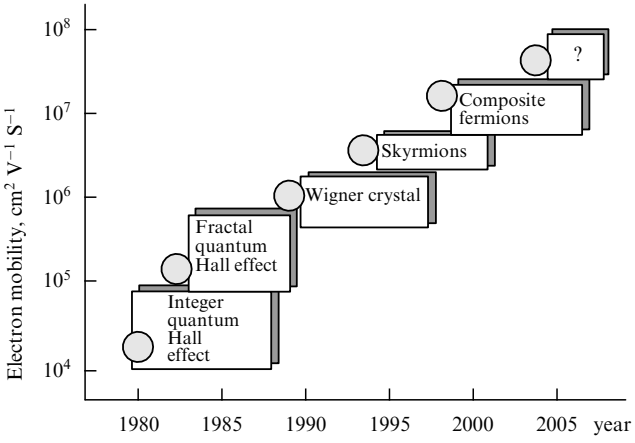

Figure 1. The succession of correlation phenomena that were discovered in the system of strongly interacting 2D electrons as electron mobility increased.

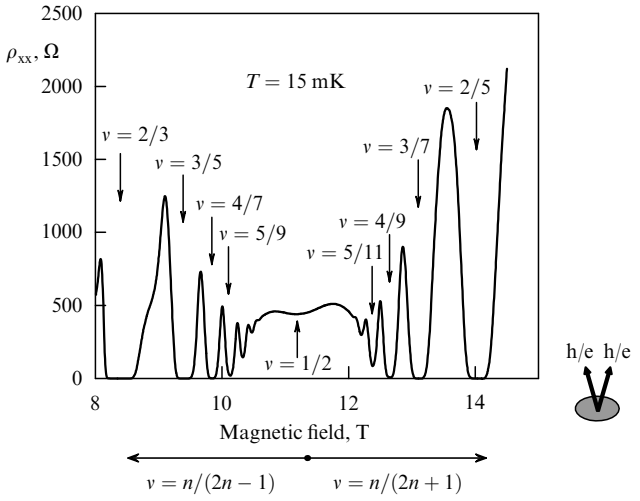

Figure 2. Shubnikov oscillation in magnetoresistance near the filling factor $\nu = 1/2$ (from Kukushkin et al. [3]). Each electron near this filling factor captures two magnetic flux quanta as shown schematically by arrows on the right.

interacting composite fermions in an effective — and weaker — magnetic field B^*,

$$B^* = B - 2pN\phi_0\,, \tag{1}$$

where $\phi_0 = h/ec$ is the magnetic flux quantum and $2p$ is an even integer. An equivalent way to say this is that electrons at a filling factor ν convert into composite fermions with the filling factor $\nu^* = N\phi_0/|B^*|$, where ν and ν^* are related by

$$\nu = \frac{\nu^*}{2p\nu^* \pm 1}\,. \tag{2}$$

Here, the minus sign is for B^* directed antiparallel to the magnetic field B. In Fig. 2, typical Shubnikov oscillations of the diagonal component of magnetoresistance near the filling factor $\nu = 1/2$ are shown, which illustrate a striking symmetry in the positions of the family of odd-denominator fractions, fully in agreement with Eqn (2) if the integer $p = 1$.

In microscopic terms, composite fermions arise as follows. We first consider the case of strongly interacting electrons in a transverse magnetic field B. With each electron, we associate an infinitely thin zero-mass solenoid carrying $2p$ quanta of magnetic flux (p being an integer, with the flux antiparallel to the field B). This procedure gives rise to composite fermions. We note that the minus sign due to the exchange interaction of two fermions remains unchanged by this conversion because the bound state of an electron with two magnetic field quanta is a fermion itself. From this fact, the composite fermion has actually derived its name. An essential point to note is that the Aharonov – Bohm phase factor remains unchanged for any closed trajectory in this conversion (the extra phase factor due to the flux $\phi = 2p\phi_0$ is $\exp\{2\pi i\phi/\phi_0\} = 1$ for such conversion). In other words, an even-flux-quanta capture by an electron is an unobservable event microscopically.

According to current views, because a new gauge field arises in an ideal 2D system [2], the Hamiltonian of the system of 2D electrons coupled to the Chern – Simons field can be written as

$$\hat{H} = \sum_i \frac{|\mathbf{p}_i + \mathbf{A}_i + \mathbf{a}_i|^2}{2m} + \frac{1}{2}\sum_{i,j} V(\mathbf{r}_i - \mathbf{r}_j)\,, \tag{3}$$

where

$$\mathbf{a}_i = \bar{\phi}\sum_{i<j} \frac{\mathbf{z}\times(\mathbf{r}_i - \mathbf{r}_j)}{|\mathbf{r}_i - \mathbf{r}_j|^2}\,.$$

The magnetic field associated with this gauge potential is

$$\mathbf{b}(\mathbf{r}) \equiv \operatorname{rot}\mathbf{a}(\mathbf{r}) = 2N\bar{\phi}\sum_j \delta(\mathbf{r} - \mathbf{r}_j)\,. \tag{4}$$

In the mean-field approximation,

$$b \to \langle b\rangle = 2p\bar{\phi}_0 N\,,$$

where $\bar{\phi}_0 = hc/e$, leading straightforwardly to expression (1).

The question naturally arises, what ultimately is the benefit of introducing the concept of composite fermions? The answer is as follows: within the mean-field approximation, the flux quanta captured by electrons create the magnetic field $-2pN\phi_0$ as a result of area averaging, leading to the residual field B^* (or field decrement) in Eqn (1). Thus each electron captures an even number $2p$ of magnetic flux quanta from the externally applied magnetic field — to become a composite fermion, which responds only to the residual field B^*.

An important point related to this (Chern – Simons) gauge transformation is noteworthy here. The multiparticle (multi-electron) ground state at $\nu < 1$ is highly degenerate in the absence of interaction because all the diversity of electron configurations for the lowest Landau level correspond to the same energy. As a result of the gauge transformation, however, the ground state of a composite fermion at $\nu^* > 1$ becomes much less degenerate even in the absence of interaction. For integer values of ν^*, the ground state simply becomes nondegenerate. With the degeneracy removed, there is every reason to treat composite fermions as noninteracting quasiparticles. Within this approximation, composite fermions fill their own Fermi sea when the effective magnetic field $B^* = 0$ (or $1/\nu = 2p$) [2]. When the effective magnetic field is nonzero (i.e., the decrement $B^* \neq 0$), composite

fermions are Landau-quantized, leading to the integer quantum Hall effect of noninteracting composite fermions. Thus, the integer quantum Hall effect of noninteracting composite fermions in the effective magnetic field is equivalent to the fractional Hall effect of strongly interacting two-dimensional electrons in the total transverse magnetic field.

We now discuss optical detection of the cyclotron resonance of composite fermions — a method that has provided the most direct way to measure the effective masses of these quasiparticles, as well as to trace how these masses depend on the inter-particle interaction (or more precisely, on the density of 2D electrons) [3, 4]. In formulating this problem, a question arises related to Kohn's theorem that in a translationally invariant system, electromagnetic radiation interacts only with the center of mass of the system and does not affect its other internal degrees of freedom. This implies that inter-particle interaction effects, expected to be strongest at large transfer momenta, cannot show up near $K = 0$. This problem can be overcome by somehow violating the translational invariance, thus enabling cyclotron transitions to be observed at large enough transfer momenta (much in excess of light momenta). Kukushkin and his coworkers [3] achieved this in their experiments by using gigahertz radiation, which generated piezoacoustic waves in the structures they studied.

We first note that the cyclotron and plasma modes hybridize in a 2D electron system of a finite size in a transverse magnetic field (analogous to the Alfven waves in three dimensions) — with the result that the frequency of the resulting magnetoplasma resonance depends in some way on the magnetic field, the concentration of the 2D electrons, and the size of the structure. For example, for a disk of diameter d, the upper and lower magnetoplasma modes have the frequencies

$$\omega_{\mathrm{DMR}}^{\pm} = \pm\frac{\omega_{\mathrm{CR}}}{2} + \sqrt{\omega_{\mathrm{P}}^2 + \left(\frac{\omega_{\mathrm{CR}}}{2}\right)^2}, \qquad (5)$$

where $\omega_{\mathrm{CR}} = eB/m^*$ is the cyclotron frequency and

$$\omega_{\mathrm{P}}^2 = \frac{3\pi^2 Ne^2}{4m^*\varepsilon_{\mathrm{eff}}\, d} \qquad (6)$$

is the plasma frequency of 2D electrons ($\varepsilon_{\mathrm{eff}} = (1+\varepsilon_0)/2$ is the effective dielectric constant and m^* is the effective mass). With the optical detection method developed by Kukushkin et al. [3] for such a hybrid, the dimensional, magnetoplasma cyclotron resonances proved to be almost two orders of magnitude more sensitive compared to using a common bolometer to detect the absorption of microwave radiation in the cyclotron resonance mode. We now turn to the optical detection of the cyclotron resonance of composite fermions at filling factors around $\nu = 1/2$. Illustrated in Fig. 3 are the corresponding resonance peaks located symmetrically about $\nu = 1/2$. It can be seen that the peak separation increases linearly with the microwave radiation frequency. Figure 4 plots the peak positions as functions of the magnetic field decrement using this as an abscissa to better show the symmetric arrangement of the peaks. The point to be made is that the linear dependence of resonance frequencies on the magnetic field decrement extrapolates exactly to $B^* = 0$ ($\nu = 1/2$) — irrevocable evidence that the observed resonances are directly related to the cyclotron motion of new 'interaction-dressed' quasiparticles, composite fermions. The

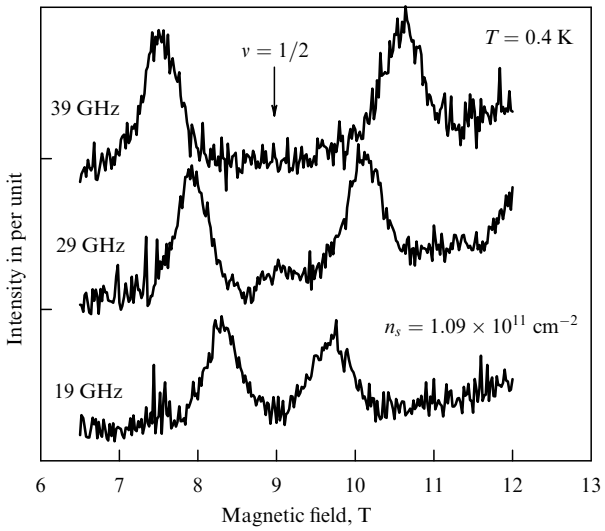

Figure 3. Cyclotron resonance of composite fermions near the filling factor $\nu = 1/2$ (From Kukushkin et al. [3]).

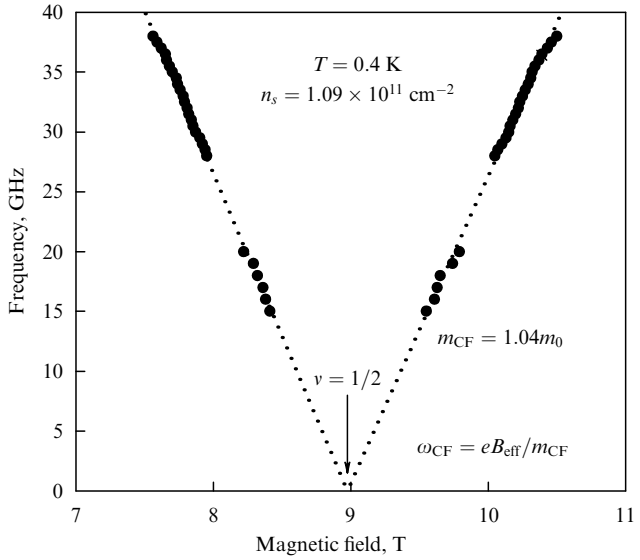

Figure 4. The linear dependence of the cyclotron resonance frequency of composite fermions on magnetic field. When linearly extrapolated, the resonance frequency dependences on the positive and negative magnetic field decrements meet very accurately at the filling factor $\nu = 1/2$ (from Kukushkin et al. [3]).

estimated mass of composite fermions is nearly an order of magnitude larger than of an electron in GaAs. Because of the inter-particle interaction, the mass of a composite particle increases as the density or magnetic field increases (Fig. 5). For an ideal 2D system, $m_{\mathrm{cr}}^{\mathrm{CF}}/m_0 = 0.079B^{1/2}$ according to numerical calculations. Experimental observations, while in qualitative agreement, are quantitatively at strong odds with theoretical expectations.

As a further essential point, whereas activation magnetotransport yields Coulomb gaps for high transfer momenta, the optical detection of cyclotron resonance involves gap measurement near $K \approx 0$. At temperatures $T > 1$ K, activation acts to destroy the construction of a composite fermion as shown in Ref. [4].

The question remains, however, to what extent may composite fermions be treated as noninteracting particles?

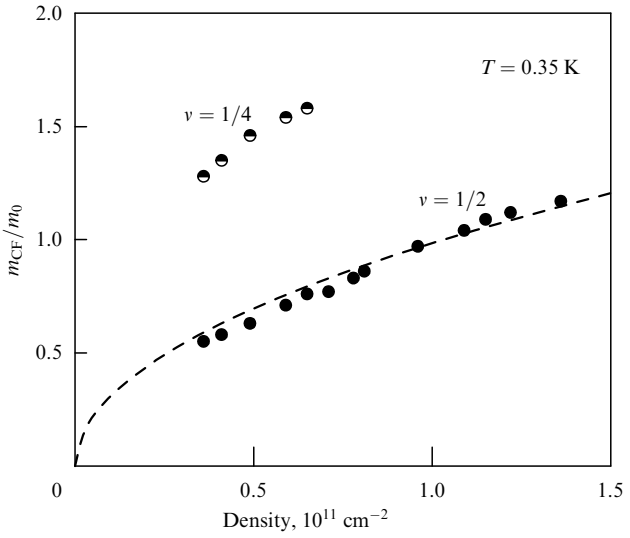

Figure 5. Composite fermion effective mass vs electron density for filling factors $\nu = 1/2$ and 1/4 (from Kukushkin et al. [3]).

The point is that the mean-field model underlying the concept of composite fermions is by no means an immaculate one. Of course, interacting composite fermions should lead to corrections to the already established properties and, more interesting and more important, to new correlated electron states in the composite fermion system itself. In a recent study of the fractal Hall effects of 2D electrons in structures with very high electron mobility [about 10^7 cm^2 (V s)$^{-1}$ or more], the diagonal component of the magnetoresistance revealed weak fractal states at the filling factors $\nu = 4/11, 5/13, 7/11, 4/13, 7/17$ and 5/17 [5]. These sequences of odd-denominator fractions do not fit into the standard series of integral quantum Hall effects of composite fermions ($\nu = p/(2mp \pm 1)$). In Ref. [5], these magnetotransport features were related to the fractal quantum Hall effects of composite fermions. If this interpretation is correct, then this study was one of the first to experimentally observe the effect of interaction between composite fermions.

3. Spatially separated electron – electron (electron – hole) quasi-two-dimensional layers

The outstanding properties of superfluid liquids and of superconductors are due to the presence of the Bose condensate of composite particles that contain an even number of particles in a strongly-interacting multi-particle medium. In superfluid ^{4}He, helium atoms are of and by themselves composite particles. In superconductors, Cooper pairs play a similar role. In semiconductors, excitons — band electron – hole pairs bound by the Coulomb interaction — have for about 40 years been considered promising for constructing a new class of neutral superfluous liquid. The well-known work by Keldysh and Kopaev [6] was the first to formulate the concepts of an exciton insulator and exciton superfluidity.

It has been demonstrated quite recently that a quasi-2D double-layer electron system placed in a strong enough magnetic field perpendicular to the layers is yet another candidate for superfluidity exotics [7]. In the presence of a magnetic field B, such a system exhibits a Hall plateau at $\rho_{xy} = h/e^2$ (the filling factor $\nu = 1$) if interlayer tunneling is weak. This quantum Hall state reflects the condensation of strongly interacting electrons to a quantum liquid that can be considered a superfluid exciton liquid where an electron in one layer is 'paired' with a (conduction-band) hole in the other. Precisely in which layer a given particle of such a composite boson is located cannot be said because of quantum uncertainty. At the filling factor $\nu = 1$, such a double-layer electron system can also be equivalently treated as an electron ferromagnet in which each electron is in a coherent superposition of 'pseudospin' states. An electron in one layer corresponds to pseudospin $|\uparrow\rangle$, whereas the other electron corresponds to pseudospin $|\downarrow\rangle$. The exchange interaction forces each electron into the coherent superposition $\{|\uparrow\rangle + |\downarrow\rangle \exp(i\varphi)\}$, where the phase φ is uniform and, in the case of no tunneling, arbitrary. The phase variable in this superposition is analogous to its superconductor or superfluid ^{4}He counterparts and determines the way the pseudospin magnetic moment is oriented. The spatial variations of this phase are the ultimate cause of low-frequency (or soft) excitations that arise in the system. This type of low-frequency excitation (the so-called linearly dispersive soft Goldstone mode) was recently discovered in a coupled double-layer electron system using tunneling spectroscopy [7]. Although superfluid current and Josephson phase oscillations have not yet been found in this system, all indications are that this will happen soon. It is these phenomena for which experiments in this field are looking.

One further very interesting system is that of spatially separated electron – hole layers [8] that arise in double quantum wells photoexcited in the presence of an applied electric field transverse to the layers [9 – 10] and in heterojunctions of the second kind. In such objects, one more correlation degree of freedom, the interlayer electron – hole interaction exists in addition to intralayer electron – electron correlations, giving rise to interwell excitons with a dipole moment already in the ground state. If the gas of such dipole – dipole repelling excitons is sufficiently dilute (the dimensionless parameter $r_S \gg 1$), then the excitons Bose-condense in lateral traps, provided the latter have somehow been prepared [11] (see the phase diagram in Fig. 6). A spatially separated high-density ($r_S \leqslant 1$) electron – hole system in a magnetic field can transform to new types of stable

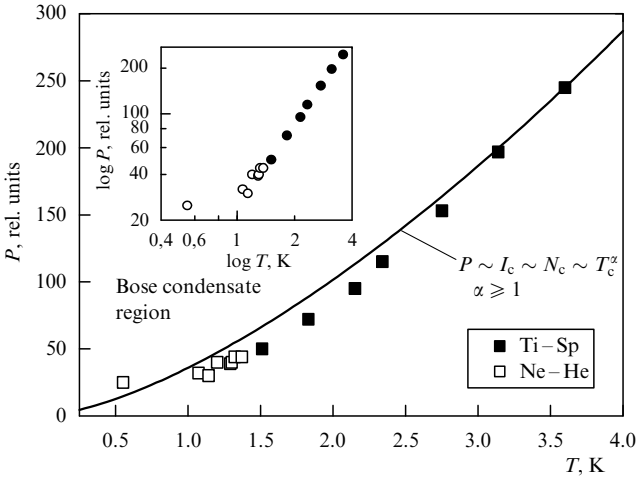

Figure 6. Phase diagram for the region of the Bose condensate of interwell excitons in lateral traps in double quantum dot GaAs/AlGaAs heterostructures (from Dremin et al. [11]).

phases: a dielectric excitonic liquid (a state of the excitonic dielectric type) and a double-layer electron – hole crystal.

4. Multi-excitonic energy levels and their symmetry in a quantum dot

The emission spectra of quantum dots and quantum dot lasers are determined by the radiative recombination of Coulomb-correlated electron – hole pairs, or excitons, that fill corresponding states (shells) in confinement conditions. The essential things to know are how the multi-particle electron – hole states in a quantum dot are constructed; in what way their filling proceeds as the number N of electron – hole pairs increases; what electron – hole configurations are most stable in the quasi-equilibrium conditions; and finally — and most important in practical terms — as excitons annihilate, what their luminescence spectra look like depending on the population of the particular states from which they originate. Given the diversity of the geometries and symmetries that a real quantum dot confinement (or confining potential) may have, these are questions for which absolutely universal answers are hardly available. One further point is that although 'artificial atoms' is a firmly established term for quantum dots in semiconductors, there are fundamental differences between these quantum objects and real atoms. In atoms, the spherically symmetric confining potential is Coulombic, determined by the positively charged nuclear core, whereas the semiconductor quantum dot confinement, which holds carriers within a given geometric scale limit, is determined by energy band discontinuities at heteroboundaries and is highly diverse in geometry and symmetry terms. Further, in electrically neutral quantum dots, unlike in atoms, the electron and hole shells are filled simultaneously as the number of excitons increases. In this respect, the way the shells are filled by electron – hole pairs in quantum dots is more reminiscent of multi-exciton complexes in multi-valley semiconductors (see, e.g., Ref. [12]).

The symmetry properties of multi-exciton configurations in a quantum dot must obey a general principle analogous to Hund's rule, well-known in atomic spectroscopy. We recall that this rule determines which of the multi-electron configurations in an atom is the optimum and most stable for the purpose of forming the ground state [13]. However, unlike in atoms, shells in a quantum dot are filled simultaneously by two types of carriers, electrons and holes.

The internal symmetry of the system of multi-exciton complexes in quantum dots essentially manifests itself in the fact that the energy of the multiplicative shell state varies close to linearly with the number of excitons on the shell,

$$E_N \cong NE_X .$$

The important implication is that the change in energy due to an exciton added to (or removed from) a shell of a particular symmetry (s-, p-, d-, etc.) does not depend on the filling of the shell and is equal to the exciton energy [14, 15].

The dynamics of the polarization operator describing interband optical transitions, $P^+ = \sum_i c_i^+ p_i^+$, suggest the same conclusion. The operator P^+ creates an electron – hole pair as a result of photon absorption, and P^- creates a photon as a result of the annihilation of an electron – hole pair. For degenerate shell states and symmetric inter-particle Coulomb interactions ($V_{ee} = V_{hh} = -V_{eh}$), the commutator assumes the simple form $[H, P^+] = +E_X P^+$, where E_X is the energy of the exciton in the shell. According to the commutator relation above, a coherent multiplicative state of N electron – hole pairs $|N\rangle = (P^+)^N|0\rangle$ is an eigenstate of the Hamiltonian, immediately implying that the energy of a multiplicative state varies linearly with the number of excitons in the shell.

For spherically or axially symmetric quantum dots, in the absence of external influences, active states are those with the angular momentum projections ± 1. When two quantum dots bind into a molecule and the axial symmetry is broken, the states of the optically active and optically inactive excitons mix to form a complex coherent superposition of states with the angular momentum projections ± 1, ± 2 (Fig. 7). Therefore, the picture of the multiplet spin splitting of a molecule in a magnetic field has nothing in common with what doublet

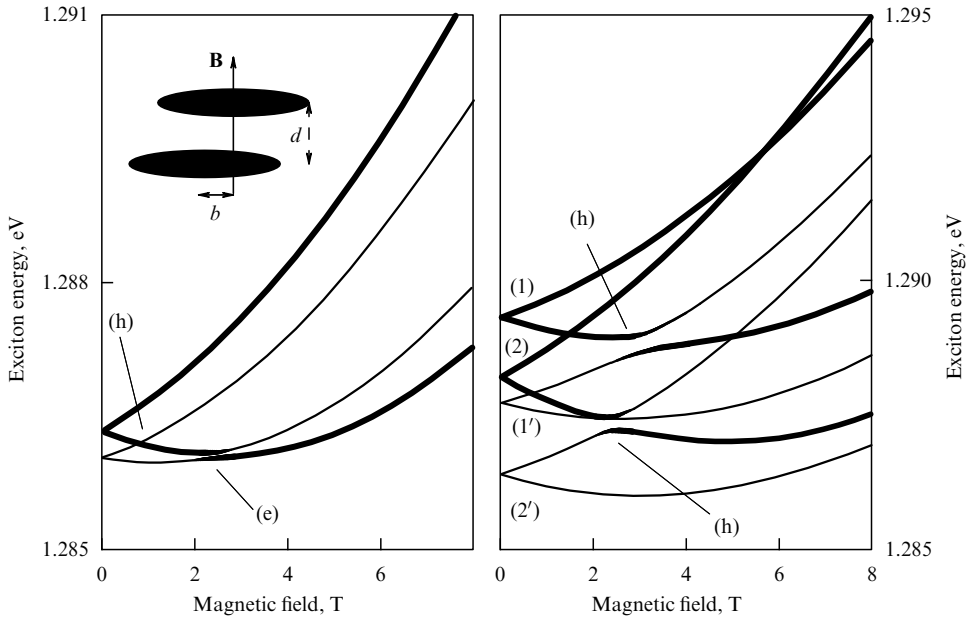

Figure 7. On the left, the expected Zeeman splitting of optically active excitons in a single quantum dot. (On top, two vertically bound quantum dots are shown schematically.) On the right, spin splitting of the ground exciton state of two quantum dots vertically bound into a molecule (calculated).

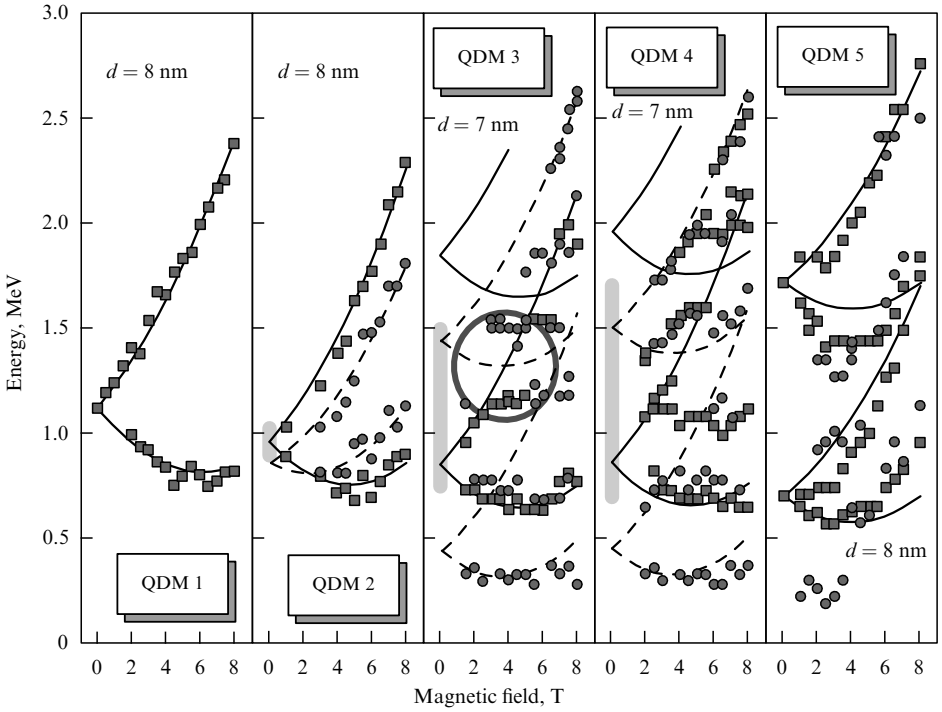

Figure 8. Experimentally measured spectra from the spin-split ground exciton state of a single quantum dot (two leftmost panels) and of two quantum dots vertically bound into a molecule (three panels on the right).

splitting or the linear Zeeman effect customarily look like for a symmetric quantum dot. Quantum molecules in a magnetic field present a complex picture of the anticrossing of mixed (entangled) spin states, the total number of multiplet components being equal to the original number of interfering spin states (Fig. 8). These observations point to the coherent mixing of spin exciton states in quantum dots bound into a molecule [16].

5. Two-dimensional exciton polaritons in microcavities

The concept of exciton polaritons has a history of nearly half a century [17]. Polaritons are stable eigenstates of excitons and photons in bulk semiconductors. Due to the translational symmetry of 3D crystals, exciton and photon states are strongly coupled for any value of the wave vector and split into an upper and a lower polariton branch near the exciton resonance. But because the lifetime of photons in a bulk crystal is determined by the mean free path of polaritons and because sufficiently low crystal perfection and low temperature make exciton scattering negligible, polaritons do not break up in the bulk of a crystal. That is, when an external photon creates an exciton in the crystal's bulk, then in the case of no scattering, the excitation oscillates between photon and exciton states (Rabi oscillations), with no irreversible processes of spontaneous radiative decays taking place. Importantly, exciton polaritons transform to external photons only near the surface of the crystal, which constitutes the main complication in the study of exciton polaritons in bulk crystals.

Two-dimensional exciton polaritons in resonant microcavities differ strongly from their bulk counterparts [18]. In a cavity, photon and exciton states are discrete due to the spatial quantization in the growth direction of the structure, and there is a 1 : 1 correspondence in k-space between photon and exciton states that are strongly coupled due to the quality of the cavity. However, because of the presence of transparent mirrors, the cavity photons have a finite lifetime in the growth direction. Therefore, polaritons turn out to be linked in the most direct way to external photons, enabling polariton states in the strong-coupling regime to be studied directly in optical experiments such as photoluminescence, reflection, and transmission. Because of dimensional quanti-

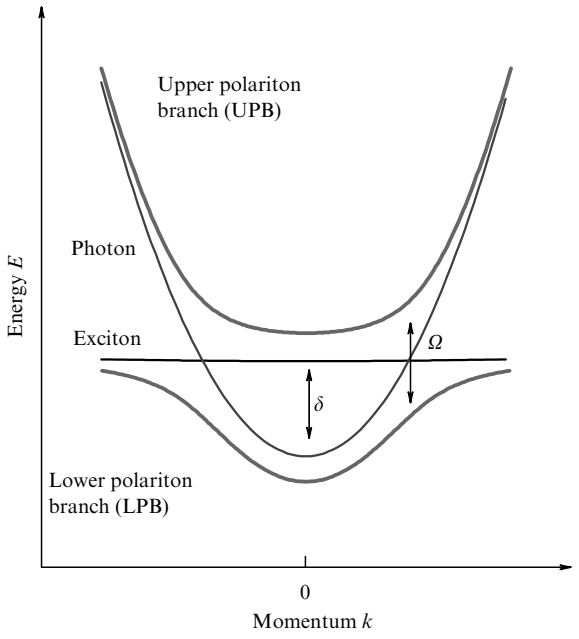

Figure 9. The upper and lower dispersion branches of two-dimensional exciton polaritons in a microcavity.

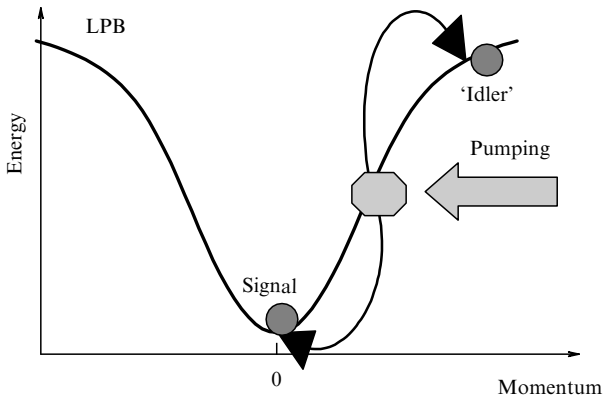

Figure 10. Parametric scattering of two-dimensional exciton polaritons under conditions of monochromatic laser pumping (schematic). The effect is strongest for the resonance laser excitation directly to the inflection point of the lower polariton branch, where the density of states is a maximum.

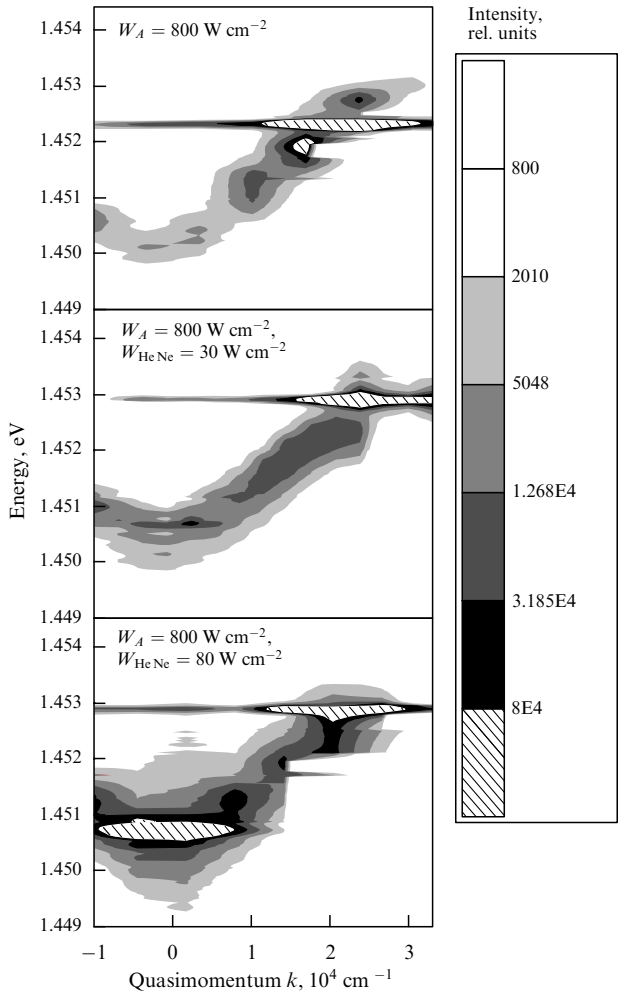

Figure 11. Development of stimulated polariton–polariton scattering. Because of stimulated scattering, two-dimensional exciton polaritons accumulate at the bottom of the band and stimulated scattering develops along the normal to the microcavity plane (from Refs [19, 20]).

zation in a cavity, photon dispersion in a plane is nearly parabolic, with an extremely low effective polariton mass. In the region of a strong light-exciton mixing (up to 3×10^6 cm^{-1}), the exciton polaritons of the lower polariton branch also have very low effective mass on the scale of $10^{-5}m_0$ (m_0 is the free electron mass, Fig. 9). Using monochromatic pumping, such exciton polaritons, which are in effect composite bosons, can be accumulated in states with a fixed and well-defined wave vector, thus achieving the macroscopic filling of the corresponding coherent state (with filling factors much larger than unity). The excitation of a nonequilibrium coherent Bose–Einstein condensate (or, in other words, of a coherent state of exciton polaritons with large filling factors, $v = 10^2$) was achieved in experiments by V D Kulakovskiĭ and his team using four-wave mixing and stimulated intraband scattering [19, 20]. The schematic of the experiment is shown in Fig. 10, and the fact itself of exciton polaritons accumulating at the bottom of a band is illustrated in Fig. 11.

6. Conclusion

It may be appropriate to conclude with a dictum allegedly coined by William Shockley, co-discoverer of the semiconductor transition, to the effect that scientific success is factorial with (rather than simply proportional to!) the number of concepts or ideas the researcher works with simultaneously. Given the quality and number of the concepts that have been established and verified, and considering the impressive pace of progress in this area of condensed matter physics, there are certainly a lot of surprises in store from fundamental research into the electron correlations in quantum-dimensional semiconductor systems and nanostructures. It is surely down the road that the most interesting things are awaiting us.

Acknowledgements. The author thanks V D Kulakovskiĭ, V D Kukushkin, and R A Suris for helpful discussions and suggestions during the writing of this brief review.

References

1. Jain J K *Phys. Rev. Lett.* **63** 199 (1989); *Adv. Phys.* **41** 105 (1992)
2. Halperin B I, Lee P A, Read N *Phys. Rev. B* **47** 7312 (1993)
3. Kukushkin I V et al. *Nature* **415** 409 (2002)
4. Kukushkin I V, in *Strongly Correlated Fermions and Bosons in Low-Dimensional Disordered Systems* (NATO Science Series, Ser. II, Vol. 72, Eds I V Lerner et al.) (Dordrecht: Kluwer Acad. Publ., 2002) p. 185
5. Pan W et at. *Phys. Rev. Lett.* **90** 016801 (2003)
6. Keldysh L V, Kopaev Yu V *Fiz. Tverd. Tela* **6** 2791 (1964) [*Sov. Phys. Solid State* **6** 2219 (1964)]
7. Spielman I B et al. *Phys. Rev. Lett.* **87** 036803 (2001)
8. Lozovik Yu E, Yudson V I *Pis'ma Zh. Eksp. Teor. Fiz.* **22** 556 (1975) [*JETP Lett.* **22** 274 (1975)
9. Fukuzawa T, Mendez E E, Hong J M *Phys. Rev. Lett.* **64** 3066 (1990)
10. Butov L V et al. *Phys. Rev. Lett.* **73** 304 (1994); *Phys. Rev. B* **59** 1625 (1999)
11. Larionov A V et al. *Pis'ma Zh. Eksp. Teor. Fiz.* **75** 689 (2002) [*JETP Lett.* **75** 570 (2002); Dremin A A et al. *Pis'ma Zh. Eksp. Teor. Fiz.* **76** 526 (2002) [*JETP Lett.* **76** 450 (2002)]
12. Kulakovskiĭ V D, Pikus G E, Timofeev V B *Usp. Fiz. Nauk* **135** 237 (1981) [*Sov. Phys. Usp.* **24** 815 (1981)]
13. Hund F *Linienspektren und periodisches System der Elemente* (Struktur der Materie in Einzeldarstellungen, Bd. 4) (Berlin: J. Springer, 1927)
14. Hawrylak P *Phys. Rev. B* **60** 5597 (1999)
15. Bayer M et al. *Nature* **405** 923 (2000)
16. Ortner G et al. *Phys. Rev. Lett.* **90** 086404 (2003)
17. Pekar S I *Zh. Eksp. Teor. Fiz.* **33** 1022 (1957) [*Sov. Phys. JETP* **6** 785 (1958)]; Hopfield J J *Phys. Rev.* **112** 1555 (1958)

18. Weisbuch C et al. *Phys. Rev. Lett.* **69** 3314 (1992)
19. Krizhanovskii D N et al. *Phys. Rev. B* **66** 165329 (2002)
20. Kulakovskiĭ V D et al. *Usp. Fiz. Nauk* **173** 995 (2003) [*Phys. Usp.* **46** 967 (2003)]